Original Article

Evaluation of liver function using hepatocyte uptake and T1 mapping indices in gadoxetic acid-enhanced magnetic resonance imaging: correlation with the albumin-bilirubin grading system

Xin Li[1#^], Guangyong Ai[1#^], Weijuan Chen[1], Hongyun Wu[1], Jing Fang[1], Rong Zhang[1], Ruiqi Chang[2], Jinhua Chen[1], Dajing Guo[1], Yangyang Liu[1^]

[1]Department of Radiology, the Second Affiliated Hospital of Chongqing Medical University, Chongqing, China; [2]The Center for Reproductive Medicine, Department of Obstetrics and Gynecology, the Second Affiliated Hospital of Chongqing Medical University, Chongqing, China

Contributions: (I) Conception and design: X Li, G Ai, Y Liu; (II) Administrative support: W Chen, J Chen, D Guo; (III) Provision of study materials or patients: X Li, G Ai, H Wu, Y Liu; (IV) Collection and assembly of data: X Li, G Ai, R Zhang, J Fang, H Wu, Y Liu; (V) Data analysis and interpretation: X Li, G Ai, R Chang, Y Liu; (VI) Manuscript writing: All authors; (VII) Final approval of manuscript: All authors.

[#]These authors contributed equally to the work as co-first authors.

Correspondence to: Yangyang Liu, MD. Department of Radiology, the Second Affiliated Hospital of Chongqing Medical University, No. 74 Linjiang Rd., Yuzhong District, Chongqing 400010, China. Email: liuyy@cqmu.edu.cn.

Background: Assessing liver function is crucial for managing chronic liver diseases. This study aimed to evaluate the efficacy of hepatocyte uptake and the longitudinal relaxation time (T1) mapping indices from gadoxetic acid-enhanced magnetic resonance imaging (MRI) for evaluating liver function and its correlation with the albumin-bilirubin (ALBI) grading system.

Methods: We retrospectively studied 183 patients who were grouped based on ALBI score: normal liver function (NLF), ALBI 1, ALBI 2, and ALBI 3. We calculated T1 indices and analyzed their correlation with ALBI grade, and differences among ALBI groups were evaluated. Receiver operating characteristic curves were used to assess the discriminative power of hepatocyte uptake and T1 indices for liver function groups, with significance set at $P<0.05$.

Results: Significant differences were observed in hepatocyte uptake and T1 indices across the NLF and ALBI groups ($P<0.001$). T1 value before enhancement (T1pre), T1 value after enhancement (T1post) prolonged, and rate of decrease in the T1 relaxation time ($\Delta T1$), hepatocyte uptake rate (K_{hep}) decreased with the advancement of liver function impairment, except for T1pre shortened in ALBI 3 grade. T1post (rho =0.762, $P<0.001$), K_{hep} (rho =–0.759, $P<0.001$) and $\Delta T1$ (rho =–0.673, $P<0.01$) showed strong correlations with ALBI grades. T1post and K_{hep} were superior to T1pre and $\Delta T1$ across all liver function groups not only in pairwise comparison but also in stratified analysis.

Conclusions: K_{hep} and T1post provide good diagnostic performance in distinguishing ALBI groups. T1post exhibits the highest area under the curve (AUC) when predicting lower liver function groups, whereas K_{hep} excels in predicting high-grade liver function. Gadoxetic acid-enhanced MRI with T1 mapping shows potential as a tool for assessing liver function.

Keywords: Liver function; gadoxetic acid-enhanced magnetic resonance imaging (gadoxetic acid-enhanced MRI); T1 mapping; hepatocyte uptake rate; albumin-bilirubin grade (ALBI grade)

^ ORCID: Xin Li, 0000-0001-7154-3828; Guangyong Ai, 0009-0004-8559-8490; Yangyang Liu, 0000-0002-1747-569X.

Submitted Aug 29, 2024. Accepted for publication Mar 03, 2025. Published online Mar 28, 2025.
doi: 10.21037/qims-24-1827
View this article at: https://dx.doi.org/10.21037/qims-24-1827

Introduction

Chronic liver disease or liver cirrhosis causes a heavy global burden. According to the World Health Organization (WHO), approximately 10% of the world population has chronic liver disease (1,2). The preoperative accurate assessment of liver function can significantly reduce the incidence of complications and perioperative mortality in patients. Thus, the assessment of liver function is of crucial importance for the management of chronic liver diseases.

Several approaches are used to assess the liver function before surgery, including the Child-Pugh score, the Model for End-Stage Liver Disease (MELD) score, and the indocyanine green 15min retention test (ICG-R_{15}) (3-5). The most widely used in the clinic is the Child-Pugh score (3), which can help to elucidate the severity and prognosis of chronic liver disease in order to predict the outcome of potentially curative approaches. However, this system has two subjective measures (ascites and hepatic encephalopathy), which can introduce variability in scoring (6). Recently, studies have shown that the albumin-bilirubin (ALBI) grade, with two measures from Child-Pugh score, has emerged as an alternative, reproducible, and objective measure of liver functional reserve in patients with liver tumors (7-9). It has been shown to be able to predict the survival rates, tumor recurrence, and risk of liver failure after various treatments for liver tumors (7). However, these liver function evaluation approaches cannot reflect the regional liver function.

Gadoxetic acid-enhanced magnetic resonance imaging (MRI) has emerged as a highly promising method for quantifying liver function and prediction for post-surgery complications (10-14). Gadoxetic acid [gadolinium-ethoxybenzyl-diethylenetriamine pentaacetic acid (Gd-EOB-DTPA)] is a paramagnetic liver-specific MRI contrast agent, which can be specifically taken up by functional hepatocytes through organic anion transporters that produce and excrete bile (15-17). Thus, its signal intensity and enhancement in the hepatobiliary phase can reflect the liver function. Several parameters, such as signal intensity, relative enhancement, relative enhancement index, biliary-to-paravertebral muscle signal-to-intensity ratio, liver-to-spleen signal intensity ratio, and functional liver imaging score have shown good diagnostic efficacy in assessment of liver function (18-23). The longitudinal relaxation time (T1) in liver tissue can be quantified using a fast T1-mapping sequence. So, the change in the liver T1 value can be used to quantitatively assess the uptake of gadoxetic acid by the liver. Additionally, by employing the B_1 inhomogeneity-corrected T1 mapping technique, the inhomogeneity of the B_1 field is rectified, leading to more accurate T1 quantification for the quantitative assessment of liver function (24). Previous studies have explored the correlation between T1 mapping-derived parameters and hepatocyte uptake indices with the Child-Pugh score, MELD score, and ICG-R_{15} (24-26). However, limited studies have examined the T1 mapping parameters in relation to the ALBI grade (27-29). Moreover, to our knowledge, no study has investigated the hepatocyte uptake rate in association with the ALBI grade. The hepatocyte uptake rate accounts solely for the gadoxetic acid absorbed by hepatocytes, eliminating the influence of the T1 relaxation time in the extracellular space (30,31).

Therefore, this study employed the ALBI scoring system to classify liver function in chronic liver disease, and on this basis, explored the clinical value of non-invasive liver function assessment using both T1 mapping-derived parameters and hepatocyte uptake rate in gadoxetic acid-enhanced MRI combined with T1 mapping with B_1 inhomogeneity corrected T1 mapping technique. We present this article in accordance with the STROBE reporting checklist (available at https://qims.amegroups.com/article/view/10.21037/qims-24-1827/rc).

Methods

Patients

The study was conducted in accordance with the Declaration of Helsinki (as revised in 2013). The study was approved by the Ethics Committee for Human Research of the Second Affiliated Hospital of Chongqing Medical University (No. [2021]121) and the requirement for individual consent for this retrospective analysis was waived. A total of 236 patients who underwent gadoxetic acid-enhanced MRI of the liver were retrospectively recruited

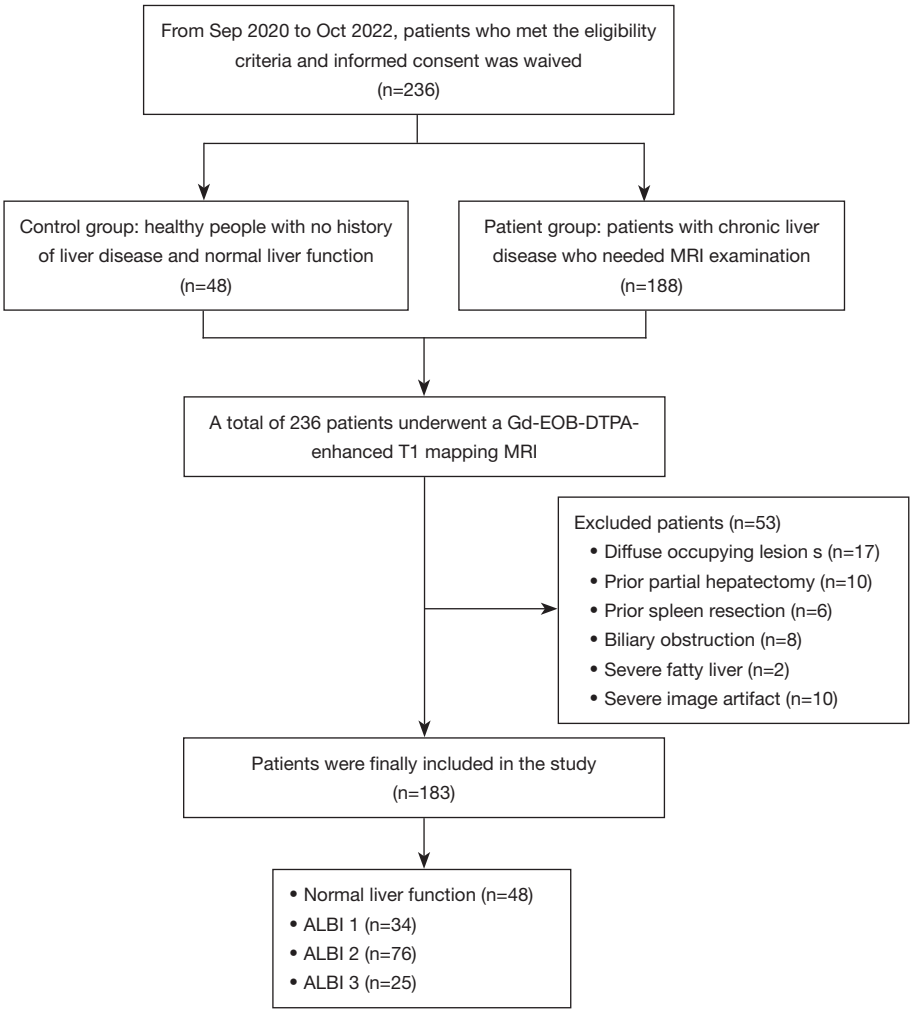

Figure 1 Flow diagram of the study population. ALBI, albumin-bilirubin; Gd-EOB-DTPA, gadolinium-ethoxybenzyl-diethylenetriamine pentaacetic acid; MRI, magnetic resonance imaging; T1, longitudinal relaxation time.

at the Second Affiliated Hospital of Chongqing Medical University from September 2020 to October 2022. The inclusion criteria were as follows: chronic B liver disease or suspected focal lesions of the liver requiring MRI. Of these patients, 53 (33 males and 20 females) were excluded due to the following reasons: (I) diffuse occupying lesions (n=17); (II) prior partial hepatectomy (n=10); (III) prior spleen resection (n=6); (IV) biliary obstruction (n=8); (V) severe fatty liver (n=2); and (VI) severe image artifact (n=10). A total of 183 patients (131 males and 52 females) were finally included (*Figure 1*). The average age of males and females was 54±12 and 57±15 years, respectively. The demographic and clinical characteristics of these patients are presented in *Table 1*. Clinical data including serum total bilirubin (TBIL) level and albumin (ALB) level were collected. ALBI grade was calculated as follows: ALBI =–0.085 × ALB (g/L) + 0.66 × Log10 TBIL (μmol/L) (7). According to the ALBI score, 48 patients had normal liver function (NLF), while 34, 76, and 25 patients were classified as ALBI grades 1, 2, and 3, respectively.

MRI protocol

The MRI examination was conducted on a 3.0T scanner (Magnetom Prisma, Siemens Healthineers, Erlangen, Germany) with a 18-channel body phased array coil and a dedicated 32-channel spinal coil. All patients underwent epigastric scanning and EOB-magnetic resonance (MR) scanning. A dose of 0.025 mmol/kg Gd-EOB-DTPA (Primovist, Bayer Schering Pharma, Berlin, Germany)

Table 1 Demographics of the study population

Parameter	Result (n=183)
Gender	
Male	131
Female	52
Age (years)	
Male	54±12
Female	57±15
Underlying disease	
Hepatitis B virus	107
Hepatitis C virus	5
Alcoholism	7
Autoimmune hepatitis	5
Others	11
History of tumors	
Primary hepatic carcinoma	66
Metastatic tumor	14
Benign tumor or tumor-like lesion	26
Mean serum markers	
Albumin (g/L)	38.00±7.00
Total bilirubin (μmol/L)	15.80±22.40
Prothrombin time (seconds)	14.60±4.00
Ascites	83 [45]

Data are conventionally expressed as mean ± standard deviation, number or number [%].

was injected intravenously at a rate of 1.0 mL/s and 20 mL of saline was administered at the same rate for tube flushing, and the T1 mapping images were acquired prior to and after 20 minutes of enhancement (hepatobiliary specific period). A rapid three-dimensional volumetric interpolated breath-hold examination (3D-VIBE) sequence was performed to obtain whole liver volume T1 mapping images in one breath-hold (13–20 s). A B_1 mapping pulse sequence was used for automatic correction before the T1 mapping sequence, according to the following T1 mapping scan parameters: flip angle 3°, 15°; inversion time 800 ms; repetition time 5.01 ms; echo time 2.3 ms; scan matrix 135×224; field of view 380 mm × 305 mm; layer thickness 4 mm; and layer spacing 0.8 mm.

Data analysis

T1 values of the liver were measured by two radiologists with 8 and 9 years of experience in liver MRI independently and blinded to the clinical information of the patients. Four regions of interest (ROIs) were placed in the left lateral lobe, left medial lobe, right anterior lobe, and right posterior lobe of the liver at the level of portal hepatis with the same size of 100 mm^2, and were labeled as ROI 1 to ROI 4, respectively (*Figure 2*). Focal lesions of the liver, major branches of bile ducts, and hepatic vessels were avoided. Two other ROIs (ROI 5 and ROI 6) were placed in the spleen at the same level. The average T1 values of the whole liver and the spleen were obtained. The average T1 values before and after the enhancement (T1pre and

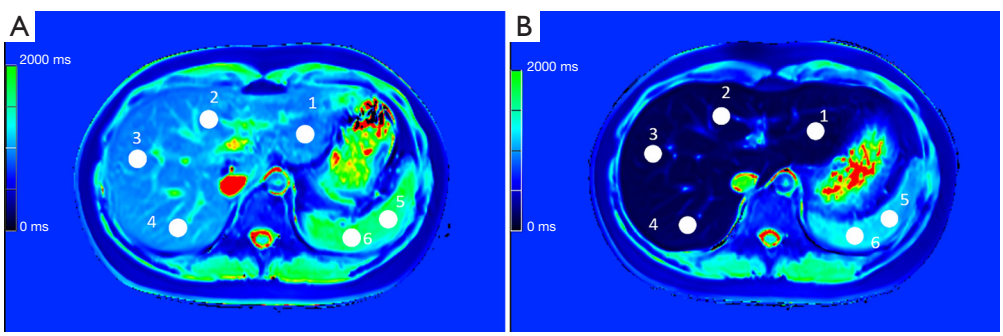

Figure 2 Schematic diagram of ROI (white circle area) selection. Male, 30 years old, with chronic hepatitis B viral hepatitis for 6 years with ALBI grade 1. (A) and (B) show the ROI selection of T1 mapping maps before enhancement and in the hepatobiliary phase, respectively. Four ROIs were placed on the medial and lateral segments of the left lobe and anterior and posterior segments of the right lobe and two ROIs on the spleen at the level of porta hepatis. ALBI, albumin-bilirubin; ROI, region of interest; T1, the longitudinal relaxation time.

T1post) of the liver were calculated. Rate of decrease in the T1 relaxation time (ΔT1) and hepatocyte uptake rate (K_{hep}) were calculated as follows: ΔT1 = (T1pre – T1post)/T1pre; K_{hep} = 0.39/20 × [(1/T1post-liver – 1/T1pre-liver)/(1/T1post-spleen – 1/T1pre-spleen) – 0.77] (26).

Statistical analysis

Statistical analysis was conducted using SPSS 23.0 software (IBM Corp., Armonk, NY, USA) and MedCalc 22.009 (MedCalc Software, Mariakerke, Belgium). The normality of measurement data was assessed using either the Kolmogorov-Smirnov or Shapiro-Wilk test. For normally distributed continuous data, descriptive statistics were presented as mean ± standard deviation, whereas non-normally distributed continuous data were described as median [interquartile range]. The inter-reader agreement between the measurements from the two radiologists was assessed using the intraclass correlation coefficient (ICC) analysis. Differences in T1 mapping indices and K_{hep} among ALBI groups were analyzed using Kruskal-Wallis one-way analysis of variance (ANOVA) in pairwise comparison. Spearman's correlation coefficient was employed to evaluate the relationships between T1 mapping indices and K_{hep} and ALBI grade. Mann-Whitney *U* test was used to compare K_{hep} and T1 mapping indices in different liver function groups [task 1: NLF *vs.* ALBI 1+2+3, task 2: NLF + ALBI 1 *vs.* ALBI 2+3, task 3: NLF + ALBI 1+2 *vs.* ALBI 3]. Receiver operating characteristic (ROC) curves were utilized to evaluate the performance of hepatocyte uptake and T1 mapping indices within each liver function group. The DeLong test was used to compare the areas under ROC. A statistically significant difference was defined as P<0.05.

Results

Comparison of the agreement of measurements between the two radiologists

The ICC values for T1pre and T1post in the liver were 0.928 and 0.987, respectively. For the spleen, the ICC values for T1pre and T1post were 0.925 and 0.975, respectively. These values demonstrate strong agreement between the two observers.

Comparison of K_{hep} and T1 mapping (T1pre, T1post, ΔT1) indices among different groups

Statistically significant differences were found in both T1 mapping indices and K_{hep} among the NLF and the ALBI groups (P<0.001) (*Table 2*). T1pre increased from the NLF group to the ALBI 2 group, but then decreased in the ALBI 3 group (P<0.001). T1post increased significantly from the NLF to the ALBI 3 group (P<0.001), whereas ΔT1 and K_{hep} decreased significantly from the NLF to the ALBI 3 group (P<0.001) (*Figure 3*).

Through pairwise comparisons, both T1post and K_{hep} exhibited statistically significant differences between the NLF and each ALBI group (ALBI 1, ALBI 2, and ALBI 3), as well as among the ALBI groups (between ALBI 1 and ALBI 3, and ALBI 2 and ALBI 3) with P<0.05. Through pairwise comparisons, both T1post and K_{hep} exhibited statistically significant differences among all different liver function groups (including the NLF and each ALBI group), with all P<0.05. ΔT1 showed a statistically significant difference in discriminating among all different liver function groups (P<0.05) except between ALBI 1 and ALBI 2 groups. T1pre only showed a statistically significant difference in discriminating the NLF from each ALBI group (the NLF from ALBI 1 group with P=0.022, the NLF from ALBI 2 group with P<0.002, and the NLF from ALBI 3 group with P=0.04), but failed in discriminating between each ALBI group (ALBI 1 from ALBI 2 group with P=0.467, ALBI 1 from ALBI 3 group with P>0.99, ALBI 2 from ALBI 3 group with P=0.812, respectively) (*Figure 3*).

Strong correlation (rho >0.6 or <–0.6) was found between T1post and ALBI groups (rho =0.762, P<0.001), between K_{hep} and ALBI groups (rho =–0.759, P<0.001), and between ΔT1 and ALBI groups (rho =–0.673, P<0.01). Weak correlation (rho >0.2) was found between T1pre and ALBI groups (rho =0.32, P<0.001). T1pre and T1post were positively correlated with ALBI groups, whereas ΔT1 and K_{hep} were negatively correlated with ALBI groups (Figure S1).

Moreover, stratified analysis showed that T1post, ΔT1, and K_{hep} had statistically significant differences in discriminating the NLF group from the ALBI 1+2+3 group, the NLF + ALBI 1 group from the ALBI 2+3 group, and the NLF + ALBI 1+2 group from the ALBI 3 group. However, T1pre only showed a statistically significant

Table 2 Comparison of K_{hep} and T1 mapping indices among different liver function groups

ALBI group	NLF (n=48)	ALBI 1 (n=34)	ALBI 2 (n=76)	ALBI 3 (n=25)	F	P value[†]
T1pre (ms)	839 [92]	919 [97]	983 [181]	901 [196]	7.575	<0.001
T1post (ms)	223 [43]	292 [70]	361 [154]	584 [170]	71.465	<0.001
ΔT1	0.75 [0.08]	0.68 [0.09]	0.62 [0.16]	0.33 [0.22]	47.243	<0.001
K_{hep}	0.26 [0.18]	0.16 [0.09]	0.09 [0.08]	0.01 [0.03]	48.847	<0.001

Data are conventionally expressed as the median [interquartile range]. [†], for the difference in the four different groups. ALBI, albumin-bilirubin; K_{hep}, hepatocyte uptake rate; NLF, normal liver function; T1, the longitudinal relaxation time; T1pre, T1 value before enhancement; T1post, T1 value after enhancement; ΔT1, rate of decrease in the T1 relaxation time.

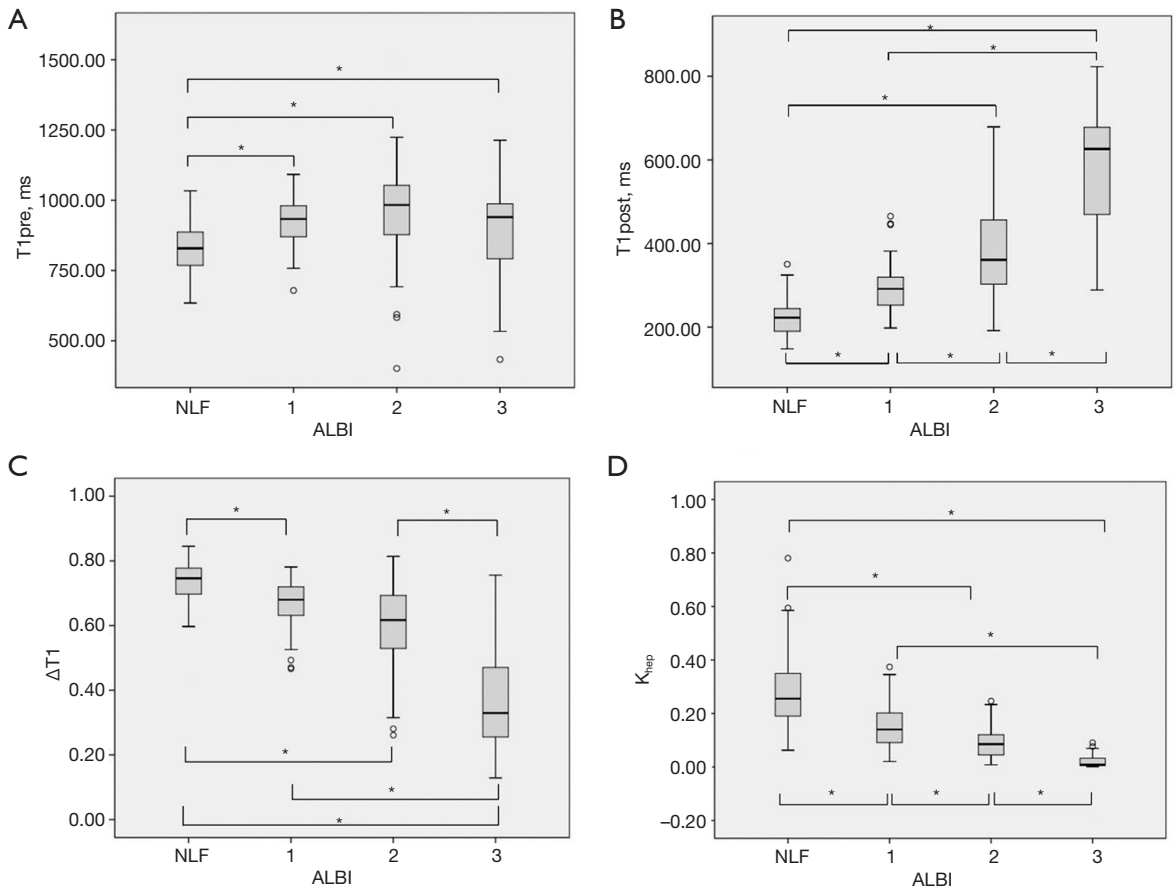

Figure 3 Boxplots of T1pre (A), T1post (B), ΔT1 (C) and K_{hep} (D) by ALBI grade. (A) T1pre increased from NLF to ALBI 2, but then decreased in ALBI 3 (P<0.001). (B) T1post increased significantly from NLF to ALBI 3 (P<0.001). (C) ΔT1 decreased significantly from NLF to ALBI 3 (P<0.001). (D) K_{hep} decreased significantly from NLF to ALBI 3 (P<0.001). *, P<0.05. ALBI, albumin-bilirubin; K_{hep}, hepatocyte uptake rate; NLF, normal liver function; T1, longitudinal relaxation time; T1post, T1 value after enhancement; T1pre, T1 value before enhancement; ΔT1, rate of decrease in the T1 relaxation time.

Table 3 Stratified analysis of different tasks

T1 indices	NLF	ALBI 1+2+3	NLF + ALBI 1	ALBI 2+3	NLF + ALBI 1+2	ALBI 3	P_1	P_2	P_3
T1pre (ms)	839 [92]	941 [156]	873 [100]	948 [172]	916 [139]	901 [196]	<0.001	<0.001	0.845†
T1post (ms)	223 [43]	403 [151]	255 [64]	438 [156]	320 [116]	584 [170]	<0.001	<0.001	<0.001
ΔT1	0.75 [0.08]	0.57 [0.16]	0.71 [0.08]	0.54 [0.17]	0.65 [0.12]	0.33 [0.22]	<0.001	<0.001	<0.001
K_{hep}	0.26 [0.18]	0.10 [0.09]	0.25 [0.17]	0.07 [0.08]	0.17 [0.15]	0.01 [0.03]	<0.001	<0.001	<0.001

Data are conventionally expressed as the median [interquartile range]. P_1: P for task 1 (NFL *vs.* ALBI 1+2+3); P_2: P for task 2 (NLF + ALBI 1 *vs.* ALBI 2+3); P_3: P for task 3 (NLF + ALBI 1+2 *vs.* ALBI 3). †, P>0.05. ALBI, albumin-bilirubin; ΔT1, rate of decrease in the T1 relaxation time; K_{hep}, hepatocyte uptake rate; NLF, normal liver function; T1, the longitudinal relaxation time; T1pre, T1 value before enhancement; T1post, T1 value after enhancement.

Table 4 Diagnostic performance of T1 mapping and hepatocyte uptake indices among different tasks by ROC curves

T1 indices	Task 1				Task 2				Task 3			
	Sensitivity (%)	Specificity (%)	Cutoff value	AUC	Sensitivity (%)	Specificity (%)	Cutoff value	AUC	Sensitivity (%)	Specificity (%)	Cutoff value	AUC
T1pre	68.89	81.25	892.72	0.75	70.3	65.85	901.36	0.69	72	44.94	890.38	0.51
T1post	81.48	93.75	275.72	0.93	90.10	74.39	278.53	0.89	76	91.14	468.55	0.89
ΔT1	68.89	89.58	0.68	0.85	65.35	91.46	0.62	0.83	88.24	52.08	0.74	0.76
K_{hep}	84.44	85.42	0.16	0.90	90.1	71.95	0.14	0.88	88.00	86.08	0.05	0.94

Task 1: NLF *vs.* ALBI 1+2+3; task 2: NLF + ALBI 1 *vs.* ALBI 2+3; task 3: NLF + ALBI 1+2 *vs.* ALBI 3. AUC, area under the curve; ALBI, albumin-bilirubin; ΔT1, rate of decrease in the T1 relaxation time; K_{hep}, hepatocyte uptake rate; NLF, normal liver function; ROC, receiver operating characteristic; T1, longitudinal relaxation time; T1pre, T1 value before enhancement; T1post, T1 value after enhancement.

difference in discriminating the NLF group from the ALBI 1+2+3 group and the NLF + ALBI 1 group from ALBI 2+3 group, but failed in discriminating the NLF + ALBI 1+2 group from the ALBI 3 group (*Table 3*).

Hepatocyte uptake and T1 mapping indices to evaluate the diagnostic efficacy in stratified analysis

For discriminating the NLF group from the ALBI 1+2+3 group, the areas under the curve (AUCs) of T1pre, T1post, ΔT1, and K_{hep} were 0.75, 0.93, 0.85, and 0.90, respectively. The largest AUC was that of T1post. However, no significant difference was found in the diagnostic performance between T1post and K_{hep} (P>0.05) (*Table 4*, *Figure 4*).

For discriminating the NLF + ALBI 1 group from the ALBI 2+3 group, the AUCs of T1pre, T1post, ΔT1, and K_{hep} were 0.69, 0.89, 0.83, and 0.88, respectively. The largest AUC was also that of T1post. The diagnostic performances of T1post, ΔT1, and K_{hep} were statistically significantly different from that of T1pre (P<0.05), whereas no statistically significant difference was found among T1post, ΔT1, and K_{hep} (P>0.05) (*Table 4*, *Figure 4*).

For discriminating the NLF + ALBI 1+2 group from the ALBI 3 group, the AUCs of T1pre, T1post, ΔT1, and K_{hep} were 0.51, 0.89, 0.76, and 0.94, respectively. The largest AUC was that of K_{hep}. The diagnostic performance of T1post, ΔT1, and K_{hep} was statistically significantly different from that of T1pre (P<0.05), and the diagnostic performance of K_{hep} was found statistically significantly different from that of T1post (P<0.05) (*Table 4*, *Figure 4*).

Discussion

Our study aimed to explore the correlation of T1-derived parameters and K_{hep} with liver function in gadoxetic acid-enhanced MRI applying B_1 inhomogeneity-corrected T1 mapping. The results showed that all examined parameters, including T1pre, T1post, ΔT1, and K_{hep} exhibited significant differences between the NLF and each ALBI group. T1post and K_{hep} were superior to T1pre and ΔT1 across all liver function groups, not only in pairwise comparison but also

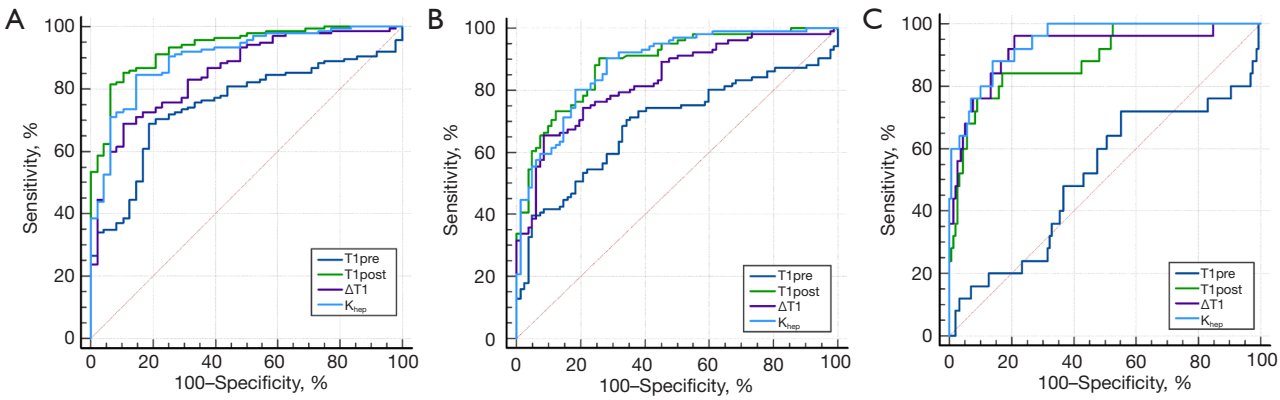

Figure 4 ROC curves of K_{hep} and T1 mapping indices to discriminate patients in different liver function groups. (A) ROC curves of discriminating the NLF from ALBI 1+2+3 group. (B) ROC curves of discriminating the NLF + ALBI 1 from ALBI 2+3 group. (C) ROC curves of discriminating the NLF + ALBI 1+2 from ALBI 3 group. ALBI, albumin-bilirubin; K_{hep}, hepatocyte uptake rate; NLF, normal liver function; ROC, receiver operating characteristic; T1, longitudinal relaxation time; T1post, T1 value after enhancement; T1pre, T1 value before enhancement; ΔT1, rate of decrease in the T1 relaxation time.

in stratified analysis. T1post demonstrated the highest AUC in distinguishing lower-grade liver function groups, whereas K_{hep} excelled in differentiating higher-grade groups. The results suggest that T1post and K_{hep} can serve as reliable non-invasive indicators for assessing liver function, as surrogates for the ALBI scoring system.

Among all T1 mapping parameters, T1post demonstrated the best performance, followed by ΔT1, and subsequently T1pre in predicting liver function. T1post not only excelled in distinguishing different liver function groups through pairwise comparison, but also demonstrated a strong correlation in stratified analysis. It yielded the highest AUCs (AUC =0.93 and 0.89) with sensitivities of 81.48% and 90.10%, respectively, along with specificities of 93.75% and 74.39%, when discriminating between lower-grade liver function groups (NLF from ALBI 1+2+3 group, and NLF + ALBI 1 from ALBI 2+3 group). These findings align with those reported by Ma *et al.*, where T1post showed significant differences between the ALBI 1 and ALBI 2+3 groups (27). The performance of T1post is also commendable in studies focusing on distinguishing among Child-Pugh groups (32) and evaluating the ICG-R_{15} >20% group (33). Given that both a Child-Pugh grade of B or higher and ICG-R_{15} >20% are viewed as contraindications to major hepatectomy (24,34), T1post emerges as a valuable supplementary diagnostic tool when deciding treatment options for hepatocellular carcinoma patients. Nevertheless, it is important to note that these findings may vary depending on the specific patient population and the type of scanner employed. Some studies have also suggested that ΔT1 outperforms other T1 mapping-derived indices (27,35).

Our study also found that K_{hep} exhibits comparable performance to T1post in distinguishing different liver function groups. Thus far, there has been no report on the assessment of liver function using hepatocyte uptake indices such as K_{hep} and hepatocyte fraction (HeF) in gadoxetic acid-enhanced MRI with T1 mapping. K_{hep} is a dual-compartment model grounded in the pharmacokinetics of the liver and spleen (30). It exclusively accounts for intrahepatocyte contrast uptake, effectively eliminating the influence of the contrast agent within the extracellular space. In a study by Bi *et al.* (33), K_{hep} demonstrated the highest AUC, sensitivity, and specificity when assessing ICG-R_{15} >20%. Moreover, Yang *et al.* (26) found that K_{hep} was superior in predicting hepatic fibrosis of grade S3 or higher.

Our research further highlighted that the AUC of K_{hep} was the highest (AUC =0.94, sensitivity =88.00%, specificity =86.08%) among all the imaging parameters when predicting high-grade liver function groups (ALBI 3 group). In contrast, T1post outperforms K_{hep} in distinguishing lower liver function grade groups. T1post was found to outperform K_{hep} in distinguishing the NLF + Child-Pugh A from the Child-Pugh B+C grade in prior research (32), which is consistent with our study. However, there is limited previous data on this quantification for patients with a more advanced or higher grade of liver function impairment, such as the ALBI 3 group or Child-Pugh C grade. Some studies

have combined the higher-grade groups due to the relatively small population with high-grade group or have even lacked information on the high-grade groups (24,27,36-39). Yet, the landscape remains underexplored, particularly in the context of studies on the Child-Pugh C grade.

The utility of T1pre in liver function evaluation has been controversial, given its poor diagnostic performance in stratifying different liver function grades. Certain studies have even abandoned its use in this context (20,22,39). Our findings illuminate a potential explanation for this suboptimal performance, as we observed a reverse diminishing trend in ALBI 3 grade after an initial increase from the NLF group to the ALBI 2 group. This observation parallels the investigations into the relationship between T1pre and the Child-Pugh classification (36), unlike some previous studies that lacked data on the higher liver function groups or grouped them together, such as ALBI 2+3 or Child-Pugh B+C, thereby missing the evolving trend (27,32,39). The converse change in trend could be attributed to the prolongation of T1 relaxation time during early liver fibrosis, driven by tissue remodeling, inflammation, and cellular edema. However, as cirrhosis advances, the T1 relaxation time shortens due to the accumulation of paramagnetic macromolecules, including iron, copper, manganese, and protein, countering the prolonged T1 relaxation time associated with liver fibrosis and resulting in a decrease in T1 relaxation time (40). Although T1pre exhibits limited capability in distinguishing between different ALBI groups, our study underscores its significant ability to differentiate the NLF group from all ALBI groups. This suggests that T1pre could serve as a viable alternative for assessing liver dysfunction without the need for contrast agents. There may also be potential for investigating segmental variations in T1pre to enhance the utility of pre-contrast T1 mapping sequences, as demonstrated by Zhou *et al.* (41), who highlighted differing abilities of various liver segments in evaluating liver function.

Our study had several limitations. We only used the ALBI score for liver function grading, without the use of MELD and ICG-R_{15} tests which have been previously investigated. Prior research also utilized the k-means cluster to categorize liver function into good and poor liver function groups based on ALBI, MELD, and ICG-R_{15} results (19). Furthermore, our analysis relied on the average T1 parameters derived from four ROIs, which might introduce bias. Additionally, our study included patients with all etiologies of chronic liver disease, which necessitates further subgroup studies.

Conclusions

K_{hep} and T1 relaxation-based index (T1post) provided good diagnostic performance for differentiation ALBI groups. T1post had the highest AUC for predicting lower liver function groups, while K_{hep} excelled for predicting high-grade liver function groups. K_{hep} and T1 relaxation-based indices based on gadoxetic acid-enhanced MRI with T1 mapping may serve as an efficient diagnostic tool for the quantitative evaluation of liver function.

Acknowledgments

We would like to thank Dr. Qi Lai (Department of Radiology, the Second Affiliated Hospital of Chongqing Medical University) for statistical support.

Footnote

Reporting Checklist: The authors have completed the STROBE reporting checklist. Available at https://qims.amegroups.com/article/view/10.21037/qims-24-1827/rc

Funding: This work was supported by the Chongqing Medical Scientific Research Project (Joint Project of Chongqing Health Commission and Science and Technology Bureau) (grant Nos. 2023QNXM029 and 2022ZDXM026).

Conflicts of Interest: All authors have completed the ICMJE uniform disclosure form (available at https://qims.amegroups.com/article/view/10.21037/qims-24-1827/coif). The authors have no conflicts of interest to declare.

Ethical Statement: The authors are accountable for all aspects of the work in ensuring that questions related to the accuracy or integrity of any part of the work are appropriately investigated and resolved. The study was conducted in accordance with the Declaration of Helsinki (as revised in 2013). The study was approved by the Ethics Committee of the Second Affiliated Hospital of Chongqing Medical University (No. [2021]121) and the requirement for individual consent for this retrospective analysis was waived.

References

1. Schuppan D, Afdhal NH. Liver cirrhosis. Lancet 2008;371:838-51.
2. Bray F, Ferlay J, Soerjomataram I, Siegel RL, Torre LA, Jemal A. Global cancer statistics 2018: GLOBOCAN estimates of incidence and mortality worldwide for 36 cancers in 185 countries. CA Cancer J Clin 2018;68:394-424.
3. Benson AB, D'Angelica MI, Abbott DE, Anaya DA, Anders R, Are C, et al. Hepatobiliary Cancers, Version 2.2021, NCCN Clinical Practice Guidelines in Oncology. J Natl Compr Canc Netw 2021;19:541-65.
4. Northup PG, Wanamaker RC, Lee VD, Adams RB, Berg CL. Model for End-Stage Liver Disease (MELD) predicts nontransplant surgical mortality in patients with cirrhosis. Ann Surg 2005;242:244-51.
5. Wang YY, Zhao XH, Ma L, Ye JZ, Wu FX, Tang J, You XM, Xiang BD, Li LQ. Comparison of the ability of Child-Pugh score, MELD score, and ICG-R15 to assess preoperative hepatic functional reserve in patients with hepatocellular carcinoma. J Surg Oncol 2018;118:440-5.
6. Sauer IM, Queisner M, Tang P, Moosburner S, Hoepfner O, Horner R, Lohmann R, Pratschke J. Mixed Reality in Visceral Surgery: Development of a Suitable Workflow and Evaluation of Intraoperative Use-cases. Ann Surg 2017;266:706-12.
7. Johnson PJ, Berhane S, Kagebayashi C, Satomura S, Teng M, Reeves HL, O'Beirne J, Fox R, Skowronska A, Palmer D, Yeo W, Mo F, Lai P, Iñarrairaegui M, Chan SL, Sangro B, Miksad R, Tada T, Kumada T, Toyoda H. Assessment of liver function in patients with hepatocellular carcinoma: a new evidence-based approach-the ALBI grade. J Clin Oncol 2015;33:550-8.
8. Demirtas CO, D'Alessio A, Rimassa L, Sharma R, Pinato DJ. ALBI grade: Evidence for an improved model for liver functional estimation in patients with hepatocellular carcinoma. JHEP Rep 2021;3:100347.
9. Hiraoka A, Kumada T, Kudo M, Hirooka M, Tsuji K, Itobayashi E, Kariyama K, Ishikawa T, Tajiri K, Ochi H, Tada T, Toyoda H, Nouso K, Joko K, Kawasaki H, Hiasa Y, Michitaka K; Real-Life Practice Experts for HCC (RELPEC) Study Group and HCC 48 Group (hepatocellular carcinoma experts from 48 clinics). Albumin-Bilirubin (ALBI) Grade as Part of the Evidence-Based Clinical Practice Guideline for HCC of the Japan Society of Hepatology: A Comparison with the Liver Damage and Child-Pugh Classifications. Liver Cancer 2017;6:204-15.
10. Verloh N, Haimerl M, Zeman F, Schlabeck M, Barreiros A, Loss M, Schreyer AG, Stroszczynski C, Fellner C, Wiggermann P. Assessing liver function by liver enhancement during the hepatobiliary phase with Gd-EOB-DTPA-enhanced MRI at 3 Tesla. Eur Radiol 2014;24:1013-9.
11. Bae KE, Kim SY, Lee SS, Kim KW, Won HJ, Shin YM, Kim PN, Lee MG. Assessment of hepatic function with Gd-EOB-DTPA-enhanced hepatic MRI. Dig Dis 2012;30:617-22.
12. Wibmer A, Prusa AM, Nolz R, Gruenberger T, Schindl M, Ba-Ssalamah A. Liver failure after major liver resection: risk assessment by using preoperative Gadoxetic acid-enhanced 3-T MR imaging. Radiology 2013;269:777-86.
13. Yu QJ, Luo YC, Zuo ZW, Xie C, Yang TY, Wang T, Cheng L. Utility of gadoxetate disodium-enhanced magnetic resonance imaging in evaluating liver failure risk after major hepatic resection. Quant Imaging Med Surg 2024;14:3731-43.
14. Breit HC, Vosshenrich J, Heye T, Gehweiler J, Winkel DJ, Potthast S, Merkle EM, Boll DT. Assessment of hepatic function employing hepatocyte specific contrast agent concentrations to multifactorially evaluate fibrotic remodeling. Quant Imaging Med Surg 2023;13:4284-94.
15. Zhou ZP, Long LL, Qiu WJ, Cheng G, Huang LJ, Yang TF, Huang ZK. Comparison of 10- and 20-min hepatobiliary phase images on Gd-EOB-DTPA-enhanced MRI T1 mapping for liver function assessment in clinic. Abdom Radiol (NY) 2017;42:2272-8.
16. Lagadec M, Doblas S, Giraudeau C, Ronot M, Lambert SA, Fasseu M, Paradis V, Moreau R, Pastor CM, Vilgrain V, Daire JL, Van Beers BE. Advanced fibrosis: Correlation between pharmacokinetic parameters at dynamic gadoxetate-enhanced MR imaging and hepatocyte organic anion transporter expression in rat liver. Radiology 2015;274:379-86.
17. Seale MK, Catalano OA, Saini S, Hahn PF, Sahani DV. Hepatobiliary-specific MR contrast agents: role in imaging

the liver and biliary tree. Radiographics 2009;29:1725-48.
18. Lee HJ, Hong SB, Lee NK, Kim S, Seo HI, Kim DU, Han SY, Choo KS. Validation of functional liver imaging scores (FLIS) derived from gadoxetic acid-enhanced MRI in patients with chronic liver disease and liver cirrhosis: the relationship between Child-Pugh score and FLIS. Eur Radiol 2021;31:8606-14.
19. Eiras-Araújo AL, Parente DB, da Silva AC, da Motta Rezende GF, Mendes GB, Luiz RR, de Oliveira Souza R, da Costa Generalis S, Rodrigues RS, Perez RM. Relative enhancement index can be used to quantify liver function in cirrhotic patients that undergo gadoxetic acid-enhanced MRI. Eur Radiol 2023;33:5142-9.
20. Dong Z, Wang M, Feng Y, Cai H, Feng ST, Li ZP, Lin Z, Peng Z. Feasibility of Imaging-Based Quantitative Hepatic Function Assessment: Gd-EOB-DTPA-Enhanced Liver MR Imaging Combined with T1 Mapping. Curr Med Imaging 2023;19:1394-403.
21. Takatsu Y, Kobayashi S, Miyati T, Shiozaki T. Hepatobiliary phase images using gadolinium-ethoxybenzyl-diethylenetriamine penta-acetic acid-enhanced MRI as an imaging surrogate for the albumin-bilirubin grading system. Eur J Radiol 2016;85:2206-10.
22. Öcal O, Peynircioglu B, Loewe C, van Delden O, Vandecaveye V, Gebauer B, Zech CJ, Sengel C, Bargellini I, Iezzi R, Benito A, Schütte K, Gasbarrini A, Seidensticker R, Wildgruber M, Pech M, Malfertheiner P, Ricke J, Seidensticker M. Correlation of liver enhancement in gadoxetic acid-enhanced MRI with liver functions: a multicenter-multivendor analysis of hepatocellular carcinoma patients from SORAMIC trial. Eur Radiol 2022;32:1320-9.
23. Kudo M, Gotohda N, Sugimoto M, Kobayashi T, Kojima M, Takahashi S, Konishi M, Hayashi R. Evaluation of liver function using gadolinium-ethoxybenzyl-diethylenetriamine pentaacetic acid enhanced magnetic resonance imaging based on a three-dimensional volumetric analysis system. Hepatol Int 2018;12:368-76.
24. Yoon JH, Lee JM, Kim E, Okuaki T, Han JK. Quantitative Liver Function Analysis: Volumetric T1 Mapping with Fast Multisection B(1) Inhomogeneity Correction in Hepatocyte-specific Contrast-enhanced Liver MR Imaging. Radiology 2017;282:408-17.
25. Kim JE, Kim HO, Bae K, Choi DS, Nickel D. T1 mapping for liver function evaluation in gadoxetic acid-enhanced MR imaging: comparison of look-locker inversion recovery and B(1) inhomogeneity-corrected variable flip angle method. Eur Radiol 2019;29:3584-94.
26. Yang L, Ding Y, Rao S, Chen C, Wu L, Sheng R, Fu C, Zeng M. Staging liver fibrosis in chronic hepatitis B with T(1) relaxation time index on gadoxetic acid-enhanced MRI: Comparison with aspartate aminotransferase-to-platelet ratio index and FIB-4. J Magn Reson Imaging 2017;45:1186-94.
27. Ma B, Xu H, Wu X, Zhu W, Han X, Jiang J, Wang Y, Yang D, Ren H, Yang Z. Evaluation of liver function using Gd-EOB-DTPA-enhanced MRI with T1 mapping. BMC Med Imaging 2023;23:73.
28. Li J, Li Y, Chen YY, Wang XY, Fu CX, Grimm R, Ding Y, Zeng MS. Predicting post-hepatectomy liver failure with T1 mapping-based whole-liver histogram analysis on gadoxetic acid-enhanced MRI: comparison with the indocyanine green clearance test and albumin-bilirubin scoring system. Eur Radiol 2024. [Epub ahead of print]. doi: 10.1007/s00330-024-11238-w.
29. Huang H, Qiao H, Jiang J, Yan J, Wen Q, Gen D, Wu Q. T1 relaxation time analysis in predicting hepatic dysfunction and prognosis in patients with HCC undergoing transarterial chemoembolization. Eur J Radiol 2023;165:110938.
30. Dahlqvist Leinhard O, Dahlström N, Kihlberg J, Sandström P, Brismar TB, Smedby O, Lundberg P. Quantifying differences in hepatic uptake of the liver specific contrast agents Gd-EOB-DTPA and Gd-BOPTA: a pilot study. Eur Radiol 2012;22:642-53.
31. Yamada A, Hara T, Li F, Fujinaga Y, Ueda K, Kadoya M, Doi K. Quantitative evaluation of liver function with use of gadoxetate disodium-enhanced MR imaging. Radiology 2011;260:727-33.
32. Liu MT, Zhang XQ, Lu J, Zhang T, Chen Q, Jiang JF, Ding D, Du S, Chen WB. Evaluation of liver function using the hepatocyte enhancement fraction based on gadoxetic acid-enhanced MRI in patients with chronic hepatitis B. Abdom Radiol (NY) 2020;45:3129-35.
33. Bi XJ, Zhang XQ, Zhang T, Xu L, Huang AN, Liu MT, Jiang JF, Chen WB. Quantitative assessment of liver function with hepatocyte fraction: Comparison with T1 relaxation-based indices. Eur J Radiol 2021;141:109779.
34. Fazakas J, Mándli T, Ther G, Arkossy M, Pap S, Füle B, Németh E, Tóth S, Járay J. Evaluation of liver function for hepatic resection. Transplant Proc 2006;38:798-800.
35. Besa C, Bane O, Jajamovich G, Marchione J, Taouli B. 3D T1 relaxometry pre and post gadoxetic acid injection for the assessment of liver cirrhosis and liver function. Magn Reson Imaging 2015;33:1075-82.
36. Katsube T, Okada M, Kumano S, Hori M, Imaoka I, Ishii K, Kudo M, Kitagaki H, Murakami T. Estimation of liver function using T1 mapping on Gd-EOB-DTPA-

enhanced magnetic resonance imaging. Invest Radiol 2011;46:277-83.
37. Kamimura K, Fukukura Y, Yoneyama T, Takumi K, Tateyama A, Umanodan A, Shindo T, Kumagae Y, Ueno S, Koriyama C, Nakajo M. Quantitative evaluation of liver function with T1 relaxation time index on Gd-EOB-DTPA-enhanced MRI: comparison with signal intensity-based indices. J Magn Reson Imaging 2014;40:884-9.
38. Lara J, López-Labrador F, González-Candelas F, Berenguer M, Khudyakov YE. Computational models of liver fibrosis progression for hepatitis C virus chronic infection. BMC Bioinformatics 2014;15 Suppl 8:S5.
39. Ippolito D, Famularo S, Giani A, Orsini EB, Pecorelli A, Pinotti E, Gandola D, Romano F, Sironi S, Bernasconi DP, Gianotti L. Estimating liver function in a large cirrhotic cohort: Signal intensity of gadolinium-ethoxybenzyl-diethylenetriamine penta-acetic acid-enhanced MRI. Dig Liver Dis 2019;51:1438-45.
40. Haimerl M, Utpatel K, Verloh N, Zeman F, Fellner C, Nickel D, Teufel A, Fichtner-Feigl S, Evert M, Stroszczynski C, Wiggermann P. Gd-EOB-DTPA-enhanced MR relaxometry for the detection and staging of liver fibrosis. Sci Rep 2017;7:41429.
41. Zhou ZP, Long LL, Qiu WJ, Cheng G, Huang LJ, Yang TF, Huang ZK. Evaluating segmental liver function using T1 mapping on Gd-EOB-DTPA-enhanced MRI with a 3.0 Tesla. BMC Med Imaging 2017;17:20.v

Cite this article as: Li X, Ai G, Chen W, Wu H, Fang J, Zhang R, Chang R, Chen J, Guo D, Liu Y. Evaluation of liver function using hepatocyte uptake and T1 mapping indices in gadoxetic acid-enhanced magnetic resonance imaging: correlation with the albumin-bilirubin grading system. Quant Imaging Med Surg 2025;15(4):3360-3371. doi: 10.21037/qims-24-1827

